Available online at www.sciencedirect.com
ScienceDirect
Journal of Photochemistry and Photobiology B: Biology 87 (2007) 183–190
Journal of Photochemistry and Photobiology B:Biology
www.elsevier.com/locate/jphotobiol

Mechanism study on the origin of delayed fluorescence by an analytic modeling of the electronic reflux for photosynthetic electron transport chain

Qiang Li, Da Xing *, Li Jia, Junsheng Wang

MOE Key Laboratory of Laser Life Science and Institute of Laser Life Science, South China Normal University, Guangzhou 510631, China

Received 7 February 2007; received in revised form 17 April 2007; accepted 18 April 2007
Available online 24 April 2007

Abstract

A mathematical–physical analysis model, which describes individually the electronic reflux of several significant components in the photosynthesis electron transport chain, was firstly developed. The process of electrons flowing back to the oxidized reaction center P_{680}^{+} was simulated by a series of photochemical reaction equations, resulting in getting the linked differential equations of delayed fluorescence (DF) intensity. MATLAB provided a computationally efficient method to solve these linked equations. Simulations based on this model showed that the decay kinetics of DF accord with double exponential. DF components decaying in the millisecond range (fast phase) are related to the charge recombination of P_{680}^{+} and Q_{A}^{-}. The components decaying in the seconds range are associated with the recombination of P_{680}^{+} with Q_{B}^{2-}. The developed model was tested in maize leaves treated with different electron blockers to induce changes in photosynthesis electron transport chain. The experimental results demonstrated that the developed model can accurately determine the regulatory effects of electron blockers on photosynthesis electron transport chain. Therefore, the model presented here could be potentially useful for studying the electron transfer in plant. It also provides an experimental workbench for testing hypotheses as to the underlying mechanism controlling the change for different phases of DF.

Keywords: Charge recombination; Decay kinetics; Delayed fluorescence; Electron blockers; Mathematical–physical analysis model

1. Introduction

Delayed fluorescence (DF) of photosynthetic organisms discovered by Strehler and Arnold [1] covers a wide time domain of many orders of magnitude (from ns to a few minutes) and depends essentially on three parameters: (i) the recombination rate of oxidizing (holes) and reducing (electrons) redox equivalents as a function of depth of their traps, (ii) the population of states with trapped electrons and holes and (iii) the quantum yield of excited singlet state formation and radiative emission [2]. Accordingly, monitoring DF provides a suitable tool to analyze the back reactions of trapped redox equivalents in photosystem (PS) II.

DF has many practical applications [3]. It can be used as a sensitive indicator for the environmental stress of artificial acid rain on zijinghua (*Bauhinia variegata* L.) and the effects of UV-B radiation on soybean (*Glycine max* Kefeng No. 1) [4,5]. Additionally, the energy conversion in photosynthesis can be evaluated by quantifying DF based on the linear correlation between the DF intensity and chlorophyll content (within a limited range) [6]. DF is more sensitive (in at least some circumstances) to stress factors than fluorescence [7]. However, the knowledge about the mechanisms of DF is far behind because of the technical complexity of delayed fluorescence registration and investigation. First, measurements of DF in short time domain bear serious problems [2]. In the paper published by Wang et al. [8], they improved

* Corresponding author. Tel.: +86 20 8521 0089; fax: +86 20 8521 6052.
E-mail address: xingda@scnu.edu.cn (D. Xing).
URL: http://laser.scnu.edu.cn/xingda.htm (D. Xing).

1011-1344/$ - see front matter © 2007 Elsevier B.V. All rights reserved.
doi:10.1016/j.jphotobiol.2007.04.005

the biosensor system for measuring DF. Now the measurements of DF signal can be achieved directly in vivo in the second range by their improved biosensor. Second, the origin of DF kinetic components is still indeterminate for the moment [9]. Though many people have described the processes of charge recombination in PS II [10–12], they presented a conceptual expression of DF only [10,11]. It brings many difficulties in further analyzing the mechanism of DF. So, it is necessary to further investigate the mechanism of electron reflux for the entire photosynthetic electron transport chain and to develop a more accurate analytical model for further investigation of DF.

From the previous work, most of the analyses on the origin of DF kinetic components focus on the primary charge separation of PS II reaction centers in the time range from microsecond to millisecond [13]. It has been reported that the decay kinetics of DF in a time range from several microseconds to milliseconds after light excitation reflect the recombination between the reduced primary quinone electron acceptor (Q_A^-) and the oxidized donor (P_{680}^+) of PS II that occurs after excitation of the reaction centers [14]. On the other hand, Turzó et al. [12] have proved that the DF components corresponding to the lifetime of 102 and 865 ms are related to the $P_{680}^+ Q_A^-$ and $P_{680}^+ Q_B^-$, respectively.

In the present study, our researches mostly focus on the time range from millisecond to second. The decay kinetics curve of leaves in the second time range can be measured using a homemade DF detection system [8]. A mathematical–physical analysis model, which describes individually the electronic reflux of several significant components in the photosynthesis electron transport chain, was firstly developed. For different electron blockers, the model can accurately reflect the regulatory effects of them on plant. The model presented here could be potentially useful for studying the electron transfer in plant. It also provides an experimental workbench for testing hypotheses as to the underlying mechanism controlling the change for different phases of DF.

2. Materials and methods

2.1. Plant material and experimental reagent

Maize was grown on compost in a phytotron (25 °C day/20 °C night) under a photo flux density of 350 μmol photons $m^{-2} s^{-1}$ (photoperiod, 12 h) supplied by incandescent lamps and fluorescent lamps (Conviron, model E7/2, Winnipeg, Canada). Leaf samples were taken from plants aged 5–8 weeks.

3-(3′,4′-dichlorophenyl)-1,1-dimethylurea (DCMU) and 1,1′-dimethyl-4,4′-bipyridyldichloride (paraquat) were purchased from Sigma. 2,5-dibromo-3-methyl-6-isopropyl-*p*-benzoquinone (DBMIB) was kindly provided by Professor Shen Yungang of the Shanghai Institute of Plant Physiology. These electron blockers were kept in dark and low temperature (4 °C). They were diluted to the concentration as needed by distilled water just before use.

All the experimental data are processed using the software ORIGIN and MATLAB in this study.

2.2. DF sensing system and DF measurements

DF emission in the time window from 0.26 to 5.26 s after being irradiated was recorded with custom-built DF biosensor system. The technical details of the system are described elsewhere [8]. Here only a brief summary of the essential parts will be presented.

Samples were irradiated by a set of light-emitting diode (LED) ($\lambda = 628$ nm, half wave width = 20 nm, single duct output luminous flux = 20 lm). The irradiance intensity was adjusted by changing the current and controlled within the range between 0 and 3000 μmol photons $m^{-2} s^{-1}$. DF was monitored at an angle of 0° with respect to the incident LEDs light. Each sample placed inside the sample chamber of the system to dark-adapt for 5 min before the irradiation source turned on. DF from the sample, immediately after the illumination period, was collected by an optical fiber bundle and transmitted to an ultra-high-sensitive Channel Photomultiplier DC-Module (CPDM (MD963, Perkin-Elmer, Wiesbaden, Germany)) with a wavelength detection range of 185–850 nm. A 660 nm long-pass filter was placed in front of the optical fiber to protect CPDM from scattered irradiation light. The output signal, which had been amplified and discriminated by the CPDM, was collected and processed by a micro control unit (MCU (AT89c55)) in the local control mode. The collected and processed signal could be storied in a memorizer (AT29c020) before further data analysis using a PC. The data collection started at 0.26 s upon the completion of the light irradiation and lasted for 5 s.

3. Theoretical model

3.1. Model

As shown in Fig. 1, during photosynthesis charge separation at PS II and PS I starts due to light absorption.

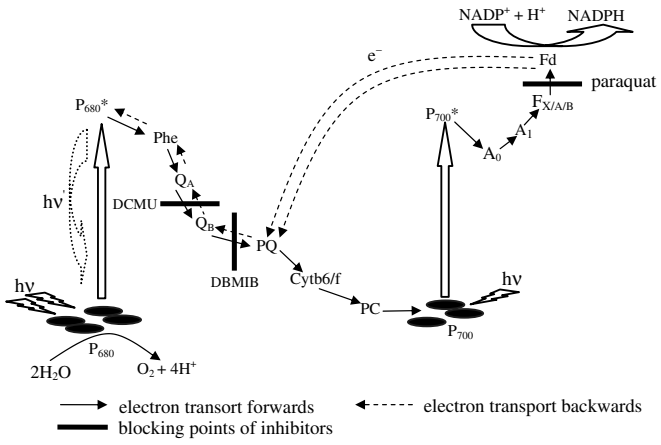

Fig. 1. Genesis of DF.

Electrons are transported through the electron transport chain from PS II to PS I. Since the rate constants of electron transport reactions in the PS I is unclear, we investigate the electron transport between P_{700} and Fd instead of considering the transfer process from P_{700} to Fd via A_0, A_1 and $F_{X/A/B}$. Then electrons transfer along the electron transport chain to the Calvin cycle.

After stopping illumination, the light phase reverses. A chain of successive inverse photochemical reactions must be realized. Considering the complicacy of the actual problems, we simplify many reactions. And it is well known that the donor side reactions should contribute to DF. However, the electron equilibrium in reaction $ZP^+ \rightarrow Z^+P$ is reached within nanoseconds [10]. Clearly, the electrons transport from the donor side to P^+_{680} is very fast. Therefore, we have reason to suppose that the donor side reactions is over by the time when electrons on the electron transport chain start to flow back to the oxidized reaction center P^+_{680}. In this case, the reactions involve:

$$2Fd^- + Q_B \underset{\leftarrow}{\overset{K_5}{\underset{K'_5}{\rightarrow}}} Q_B^{2-} + 2Fd, \tag{1}$$

$$Q_B^{2-} + 2Q_A \underset{\leftarrow}{\overset{K_4}{\underset{K'_4}{\rightarrow}}} 2Q_A^- + Q_B, \tag{2}$$

$$Q_A^- + Phe \underset{\leftarrow}{\overset{K_3}{\underset{K'_3}{\rightarrow}}} Q_A + Phe^-, \tag{3}$$

$$Phe^- + P^+_{680} \underset{\leftarrow}{\overset{K_2}{\underset{K'_2}{\rightarrow}}} P^*_{680} + Phe, \tag{4}$$

$$P^*_{680} \overset{K_1}{\rightarrow} P_{680} + h\nu, \tag{5}$$

where $K_1, K_2, K'_2, K'_3, K_3, K_4, K'_4, K_5$ and K'_5 are the rate constants of reactions, respectively. Based on the electronic reflux hypothesis of DF developed during the last decades, it is possible to determine such characteristics of primary processes as rate constants for forward electron transport reactions and for backward electron transport reactions in the photosystem reaction center [15]: $K_1 = 1\times10^{10}\ s^{-1}$, $K_2 = 9\times10^8\ s^{-1}$, $K'_2 = 4\times10^9\ s^{-1}$, $K_3 = 2\times10^3\ s^{-1}$, $K'_3 = 2\times10^9\ s^{-1}$, $K_4 = 1\times10^2\ s^{-1}$ and $K'_4 = 6\times10^3\ s^{-1}$.

(I) If we take the electronic reflux of Q_A^- alone into account after the illumination stops, Eqs. (3)–(5) must be realized. Since these rate constants of reactions K_1, K_2, K'_2 and K'_3 are far larger than K_3, using the steady state approximation and equilibrium hypothesis, we can neglect the backward reaction of Eq. (3) and get linked differential equations as follows:

$$\begin{cases} \frac{d[Q_A^-]}{dt} = -K_3[Q_A^-][Phe] \\ \frac{d[Phe^-]}{dt} = K_3[Q_A^-][Phe] - K_2[Phe^-][P^+_{680}] + K'_2[P^*_{680}][Phe] = 0, \\ \frac{d[P^*_{680}]}{dt} = K_2[Phe^-][P^+_{680}] - K'_2[P^*_{680}][Phe] - K_1[P^*_{680}] \end{cases} \tag{6}$$

where $[Q_A]$ and [Phe] are the concentration of Q_A and Phe, respectively. $[Q_A^-]$ and $[Phe^-]$ are the concentrations of reduced Q_A and Phe in the entire electron transport chain, respectively. $[P^+_{680}]$ is the concentration of oxidized P_{680}. $[P^*_{680}]$ is the concentration of excited P_{680}.

As to the certain growth period, [Phe] can be assumed as constant C_1 under determinate illumination. In this case I_{DF} can be calculated from Eq. (6):

$$I_{DF} = K_1[P^*_{680}] = K_1C_5e^{-K_1t} + \frac{K_1K_3C_1C_4}{K_1 - K_3C_1}e^{-K_3C_1t}. \tag{7}$$

where K_1 is far larger than K_3, so we can neglect the first item. Then I_{DF} can be expressed as

$$I_{DF} = \frac{K_1K_3C_1C_4}{K_1 - K_3C_1}e^{-K_3C_1t}. \tag{8}$$

(II) If we take the electronic reflux of Q_B^{2-} along into account after the illumination stops, Eqs. (2)–(5) must be realized. In the same way, using the method of steady state approximation, we can neglect the backward reactions of Eqs. (2) and (3) and get linked differential equations. $[Q_B^{2-}]$ is the concentration of reduced Q_B. As to the certain growth period, [Phe] and $[Q_A]$ can be assumed as constants C_1 and C_2 under determinate illumination, respectively. We carry out the equation group and get the expression of I_{DF} as

$$\begin{aligned} I_{DF} = {} & K_1C_8e^{-K_1t} + \frac{K_1K_3C_1C_7}{K_1 - K_3C_1}e^{-K_3C_1t} \\ & + \frac{2K_1K_3K_4C_1C_2^2C_6}{(K_3C_1 - K_4C_2^2)(K_1 - K_4C_2^2)}e^{-K_4C_2^2t}, \end{aligned} \tag{9}$$

where $[Q_B^{2-}] = C_6e^{-K_4C_2^2t}$ and $[Q_A^-] = C_7e^{-K_3C_1t} + 2K_4C_2^2C_6/K_3C_1 - K_4C_2^2e^{-K_4C_2^2t}$. So $[Q_B^{2-}]$ and C_6 are positive correlative with each other, and $[Q_A^-]$ is positive correlative with C_7. And because K_1 is far larger than K_3 and K_4, so we can neglect the first item and get the expression of I_{DF} as follows:

$$\begin{aligned} I_{DF} = {} & \frac{K_1K_3C_1C_7}{K_1 - K_3C_1}e^{-K_3C_1t} \\ & + \frac{2K_1K_3K_4C_1C_2^2C_6}{(K_3C_1 - K_4C_2^2)(K_1 - K_4C_2^2)}e^{-K_4C_2^2t} \\ \approx {} & 2\times10^3C_1C_7e^{-2000C_1t} + 2\times10^2C_2^2C_6e^{-100C_2^2t}. \end{aligned} \tag{10}$$

Expression (10) can be simplified to

$$I_{DF} = I_{10}e^{-t/\tau_1} + I_{20}e^{-t/\tau_2}, \tag{11}$$

where $\tau_1 = 1/2000C_1$, $\tau_2 = 1/100C_2^2$, $I_{10} = 2\times10^3C_1C_7$, $I_{20} = 2\times10^2C_2^2C_6$. τ_1, which is called decay rate constant of the fast decay component, is related to the excited state P^*_{680} leaded by the recombination of P^+_{680} and Q_A^-. τ_2, which is called decay rate constant of the slow decay component, is associated with the excited state P^*_{680} leaded by the recombination of P^+_{680} with Q_B^{2-}. I_{10} and I_{20}, respectively, correspond to DF intensities of different decay speeds at time t_o after illumination has ceased. Moreover, from their expressions, we can find out that I_{10} and I_{20} are, respectively, positive correlative with $[Q_A^-]$ and $[Q_B^{2-}]$.

Taking into consideration other electronic carriers in the photosynthetic electron transport chain, we can educe that the decay kinetics of DF accords with ploy-exponent. From

the previous works, however, it has been demonstrated that DF is mainly emitted from PS II [2,4]. Then if electrons of PS I flow back to the oxidized reaction center P^{+}_{700}, an excited state P^{*}_{700} will be obtained, but instead of reaching P^{+}_{680}, the energy of excited state P^{*}_{700} will be dissipated by non-photochemical quenching and other modalities. Based on the developed cyclic flow theory in recent years, we suggest that electrons of PS I should flow back to the oxidized reaction center P^{+}_{680} via cyclic electron flow [16].

Synthesizing the above analysis, we simplify the expression of DF as follows:

$$I_{DF}(t) = I_{10}e^{-t/\tau_1} + I_{20}e^{-t/\tau_2} + I_{30}e^{-t/\tau_3}, \quad (12)$$

where the third item represent the long-lived DF components leaded by the recombination of P^{+}_{680} with electrons of PS I. Because the reaction rate of the third item is very little and the route of electronic reflux is very long, we assume the rate constant τ_3 is infinitely great. Then Eq. (12) simplifies to

$$I_{DF}(t) = I_{10}e^{-t/\tau_1} + I_{20}e^{-t/\tau_2} + C, \quad (13)$$

where C represents the total of the long-lived DF components and the noise. From Eq. (13), we could say that DF decay curves could be enough to be fitted by two exponentials.

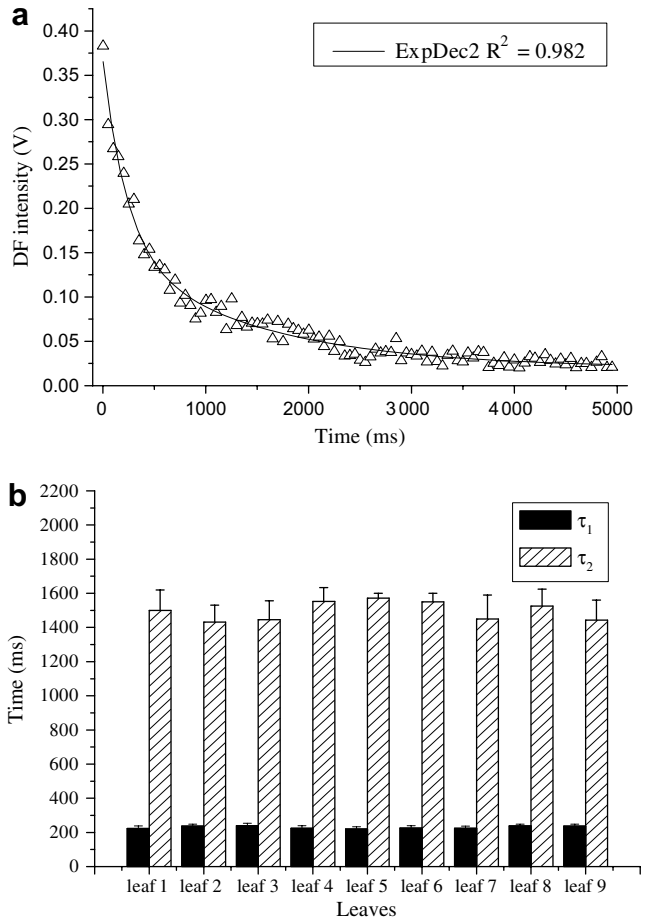

Fig. 2. (a) Decay curve of DF of leaf. The measurement was fitted by two components. (b) Statistics of τ_1 and τ_2 for different leaves, in the figure each value is the mean ± SD of five repeated experiments.

3.2. Evaluation of the rate constants τ_1 and τ_2

From Eq. (13), we can find out that the rate constants $\tau_1 = 1/2000C_1$ and $\tau_2 = 1/100C_2^2$. They are fixed for all DF decay curves of leaves. But their concrete values are unknown, so we evaluate these parameters through experimental fitting. The decay curve of leaf was measured using the homemade DF detection system (Fig. 2a). The resulting decay curve can be well fitted by two exponentials ($R^2 = 0.982$) using the software ORIGIN (The curves fitted according to the least square method principle). And the rate constants τ_1 and τ_2 are obtained to be 230 ms and 1500 ms, respectively.

In order to check up the conclusion, the DF decay curve of large numbers of maize leaves with equal size, weight and close initial light-induced DF intensity were further measured (The decay curve are not shown). These experimental curves were fitted with the model (Eq. (13)), and the values of τ_1 and τ_2 in different leaves are shown in Fig. 2b. The significant difference of τ_1 in different leaves and significant difference of τ_2 in different leaves are, respectively, evaluated by t-test. We find that for τ_1, $P_1 > 0.05$ and for τ_2, $P_2 > 0.05$. So there are no significant differences for τ_1 in different leaves and for τ_2 in different leaves.

4. Results

4.1. Effect of different concentrations of DCMU on decay curve

Leaves with equal size, close initial light-induced DF intensity and weight were measured after being submerged in different concentrations of DCMU solution for 45 min. Then we fitted the measured decay curves of DF using the model (Eq. (13)). The effects of different concentrations of DCMU on I_{10} and I_{20} were shown in Fig. 3 (The primary curves are not shown). From Fig. 3, we can find that I_{10} increases gradually from 0.2088 to 0.2958 with the increase of the concentration of DCMU. However, I_{20} reduces from 0.1246 to 0.0742 with the increase of the concentration of DCMU.

4.2. Effect of different concentrations of DBMIB on decay curve

In order to further analyze the change of electron transport chain, we repeat the above-mentioned experiments with DBMIB. The effects of different concentrations of DBMIB on I_{10} and I_{20} were shown in Fig. 4 (The primary curves are not shown). Fig. 4 shows that I_{10} and I_{20} increase gradually from 0.1915 and 0.3053 to 0.1076 and 0.1858 with the increase of the concentration of DBMIB, respectively.

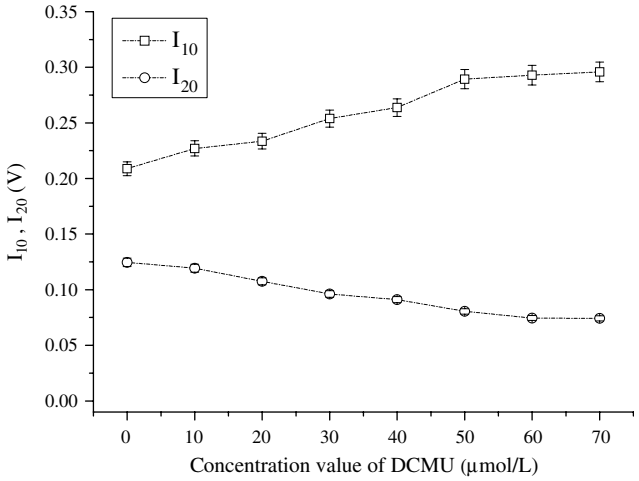

Fig. 3. Effects of different concentrations of DCMU on I_{10} and I_{20}. In the figure each value is the mean ± SD of five independent experiments.

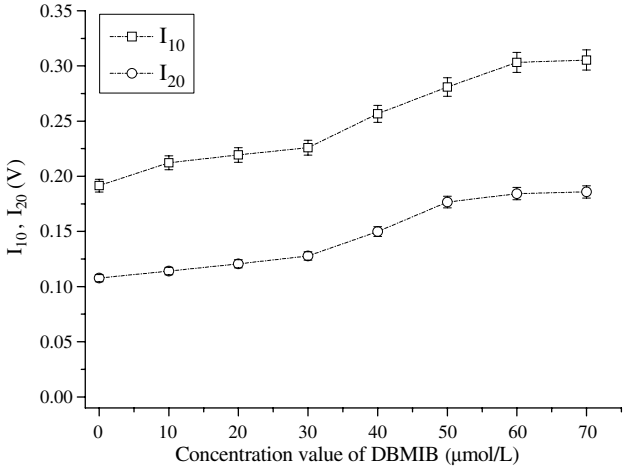

Fig. 4. Effects of different concentrations of DBMIB on I_{10} and I_{20}. In the figure each value is the mean ± SD of five independent experiments.

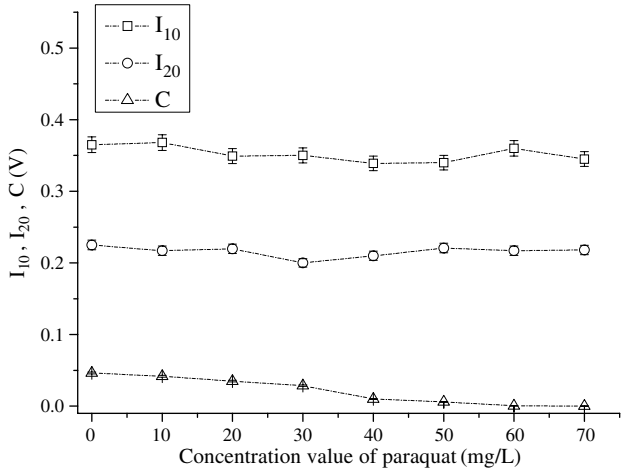

Fig. 5. Effects of different concentrations of paraqaut on I_{10}, I_{20} and C. In the figure each value is the mean ± SD of five independent experiments.

4.3. Effect of different concentrations of paraquat on decay curve

Using our developed model, we also examine the effects of different concentrations of paraquat on I_{10}, I_{20} and C. The result is shown in Fig. 5. It is clear that I_{10} and I_{20} are nearly invariable (about 0.352 and 0.216, respectively),

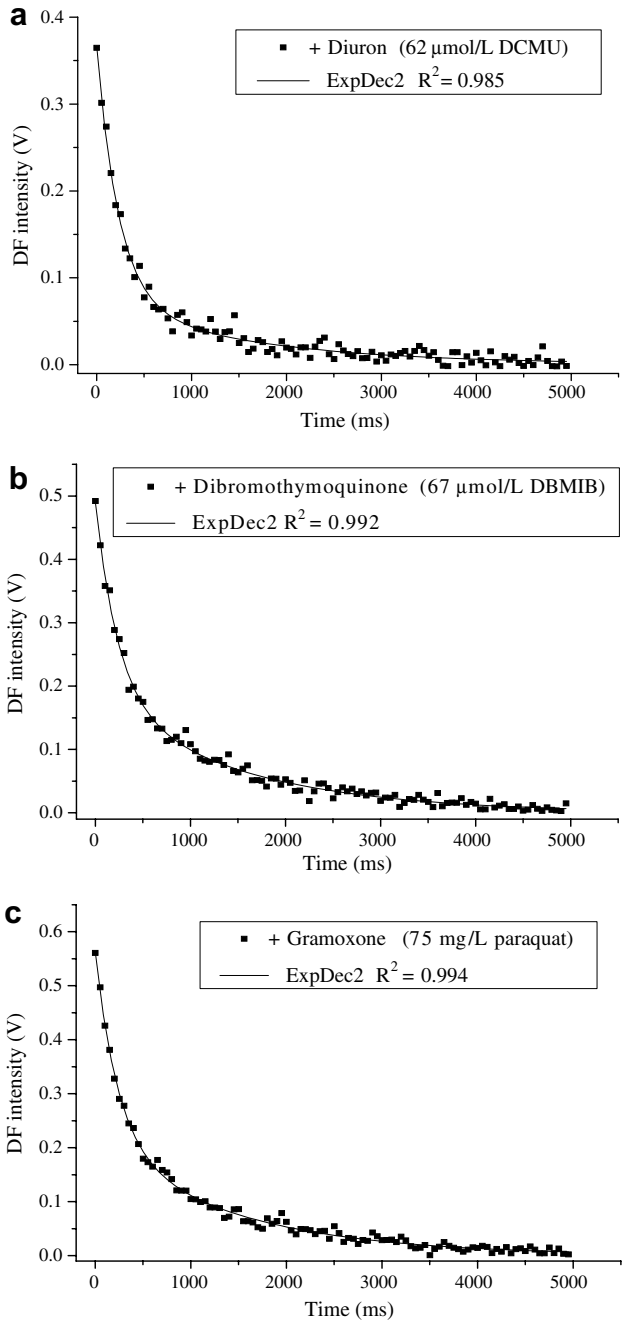

Fig. 6. Comparison of the results obtained by the model and experimental data in the presence of diuron (62 μmol/L DCMU) (a), dibromothymoquinone (67 μmol/L DBMIB) (b), gramoxone (75 mg/L paraquat) (c). In the figure each curve is the typical representation of five repeated experiments.

while C reduces gradually from 0.0463 to 0.0002 with the increase of the concentration of paraquat.

4.4. Application of model

Three kinds of common herbicides (Diuron, Dibromothymoquinone and Gramoxone) were used as experimental reagent. Their effective components are DCMU, DBMIB and paraquat, respectively. According to the concentration percentage of effective component on the label, their concentration of effective component can be worked out. After treating with these herbicides at their concentration values of effective component, the corresponding value of I_{10}, I_{20} and C can be found out in Figs. 3–5, respectively. Based on these parameter values that we have got (I_{10}, I_{20} and C), we can predict the theoretical DF decay curve of leaves treated with different herbicides. Comparing with experimental data as shown in Fig. 6, the theoretical curves and experimental curves are in good agreement (Their fitting rates (R^2) are more than 0.98).

5. Discussion

Through strict mathematic analysis, we have developed a mathematical–physical analysis model of DF (Eq. (13)). It is clear that the decay model of DF accord with two exponentials. In the model, the five related parameters (two rate constants, DF intensity of fast phase, slow phase and long-live components) have been semiquantitative expressed and further named τ_1, τ_2, I_{10}, I_{20} and C.

As seen from the model, τ_1 and τ_2 are the key factors for the two exponentials decay curve. Based on their expressions ($\tau_1 = 1/2000C_1$ and $\tau_2 = 1/100C_2^2$), they are fixed for all DF decay curves of leaves. From Fig. 2a, the concrete values of τ_1 and τ_2 are obtained to be 230 ms and 1500 ms, respectively. Moreover, we check up the conclusion in large numbers of maize leaves. The results indicate that τ_1 and τ_2 are invariable for all decay curves of maize leaves (Fig. 2b). These findings are similar to Turzó et al. [12], but different from those obtained by Itoh and Murata [14]. The primary reason is that the experiment method applied by us to measure DF is different from that by Itoh and Murata. During measuring, they divided the DF measuring process into consecutive cycles of 1 ms excitation by light followed by 4.6 ms darkness. And then they measured the DF between 1 and 3 ms after every flash with a photomultiplier. Therefore, those signals received may include some other interferential signals, such as the residual signals caused by repetition excitation, partial fluorescence signals and phosphorescence signals.

From the model, I_{10} and I_{20} have prominent influence on the DF decay kinetics too. Since I_{10} and I_{20} are, respectively, correlative with $[Q_A^-]$ and $[Q_B^{2-}]$, and since electron blockers by stopping electron transportation lead to changes of $[Q_A^-]$ and $[Q_B^{2-}]$, by applying different electron blockers to act on leaves we can do research on the model based on the changes of I_{10} and I_{20}. The DF decay curves of leaves were measured under the effects of different electron blockers. Under the effect of DCMU, through experimental fitting, we find that fast DF components (I_{10}) increases gradually with the increase of the concentration of DCMU. However, slow components (I_{20}) reduce gradually (Fig. 3). While under the effect of DBMIB, both fast DF components and slow components increase with the increase of the concentration of DBMIB (Fig. 4). This is because the mechanism of DCMU action on electron transport chain is different from DBMIB. DCMU can stop the electron transport from Q_A^- to Q_B, and accumulate the charge in Q_A during illumination [17]. Thus $[Q_A^-]$ increases, whereas $[Q_B^{2-}]$ reduces. Based on the model, I_{10} corresponding to $[Q_A^-]$ would increase, while I_{20} corresponding to $[Q_B^{2-}]$ reduces. From Fig. 3, the value of I_{20} represents the leakages of the DCMU block. Both the changes of I_{10} and I_{20} can reflect the efficiency of DCMU block. As to DBMIB, it blocks the electron transport from PQ^- to $Cytb_6/f$ [18]. The charge produced in illumination would pile up in Q_A and Q_B, which results in the increase of $[Q_A^-]$ and $[Q_B^{2-}]$. Thus I_{10} and I_{20} corresponding to $[Q_A^-]$ and $[Q_B^{2-}]$, respectively, would increase (Fig. 4). Similarly, the changes of I_{10} and I_{20} can reflect the efficiency of DBMIB block. We also observe that the values of I_{10} and I_{20} are displayed an approximate linear correlation with the concentration of electron blockers from Figs. 3 and 4. However, the accurate mathematical relationship of them still needs further investigation. In total, under the effects of different electron blockers, the changes of the model parameters (I_{10} and I_{20}) can directly reflect the changes of the electron transport chain.

Because the value of the third item of the model (Eq. (13)) is very small compared with the former two items, we consider it a constant. But considering the fact that the third item, which also affects the decay curve, includes not only the noise but also the long-lived DF components, thereupon, we further analyze the effect of paraquat on the model. As for the effect of paraquat, I_{10} and I_{20} (fast phase components and slow phase components) are nearly invariable with the increasing of the concentration of paraquat, while C reduces gradually (Fig. 5). This is because the cyclic electron transport was inhibited by paraquat. When leaf was acted by paraquat, the reduction of Fd would be inhibited [19]. Electrons transmitted to PS II via cyclic flow would decrease during illumination. But Q_A and Q_B of PS II are scarcely influenced. Therefore, I_{10} and I_{20} depended on the electronic reflux of Q_A^- and Q_B^{2-}, respectively, would not change along with the change of the concentration of paraquat. Since C includes the long-lived DF components, the fall of electrons from PS I will lead to the decrease of C. Accordingly, C would reduce gradually with the increase of the concentration of paraquat. Investigations performed herein indicate that the total DF intensity will reduce with the increase of the concentration of paraquat.

In previous reports we have demonstrated that there is a linear correlation between the DF intensity and the photo-

chemical efficiency of PS II [4]. Therefore, paraquat can decrease the photochemical efficiency of PS II. Why paraquat inhibited the activity of PS I can affect the activity of PS II? Munekage et al. [16] and Okegawa et al. [20] have presented that PS I should cooperate with PS II among the physiological processes of plant growth and development. The cyclic electron flow is an important regulator of them. Current investigations indicate that C can directly reflect the inhibitive degree of cyclic flow. But this approach must be used for more caution, considering the not negligible noise.

From Figs. 3–5, we can calculate the values of I_{10}, I_{20} and C under any concentrations of three kinds of common herbicides action. Consequently the theoretical DF decay curves of leaves treated with different herbicides can be predicted. Fig. 6 shows the results of comparing the theoretical curves with experimental curves. From Fig. 6, the experimental decay curves are in good agreement with the theoretical curves.

As seen from the above experimental results, the model can truly and quantificationally reflect the mechanism of herbicides action on photosynthetic organisms. DF of chlorophyll can be used as sensitive tool to study electron transfer in photosynthetic organisms. It also can be utilized in clarifying the mode of action of different inhibitors, testing and identifying new chemicals and potential herbicides. Based on the comparison between the results obtained by DF measurement and those by thermoluminescence (TL) [21,22], we find both methods are in-depth investigation and discussion on the electron transfer of photosynthetic organisms. Comparing with the TL method, DF method presented in this study can quantify the change of photosynthesis electron transport chain more accurately and faster under its physiological status with less interference from the environment.

6. Conclusions

In this study, a simple analytical model of DF was developed based on the charge recombination theory. The mechanism of origin of DF kinetic components of plant was also studied using a homemade DF detection system. The model successfully simulates the decay kinetics of DF, resulting in providing an experimental workbench for testing hypotheses as to the underlying mechanism controlling the change for different phases of DF. Further more, the model can accurately predict the DF decay curve of plant treated with different herbicides. Since the changes in decay curve of DF of green plants can reflect the degree of pollution resulting from herbicide toxicity, decay kinetics of DF with proper calibration may become a promisingly new means to evaluate herbicide toxicity stress on plants. Besides, the model may be used for monitoring plant damage resulting from various stresses, such as leaf ageing and high-temperature, as the changes in decay curve of DF of plants can reflect the degree of blocking of electron transfer.

7. Abbreviations

DBMIB	2,5-dibromo-3-methyl-6-isopropyl-*p*-benzoquinone
DCMU	3-(3′,4′-dichlorophenyl)-1,1-dimethylurea
DF	delayed fluorescence
Fd	ferredoxin
PC	plastocyanin
PQ	plastoquinone
Paraquat	1,1′-dimethyl-4,4′-bipyridyldichloride
PS II	photosystem II
PS I	photosystem I
Q_A	primary plastoquinone acceptor of PS II
Q_B	secondary plastoquinone acceptor of PS II
TL	thermoluminescence

Acknowledgements

This research is supported by the National Natural Science Foundation of China (30670507; 30600128; 30470494) and the Natural Science Foundation of Guangdong Province (015012).

References

[1] B.L. Strehler, W. Arnold, Light production by green plants, J. Gen. Physiol. 34 (1951) 809–820.
[2] G. Christen, R. Steffen, G. Renger, Delayed fluorescence emitted from light harvesting complex II and photosystem II of higher plants in the 100 ns–5 μs time domain, FEBS Lett. 475 (2000) 103–106.
[3] C.L. Wang, D. Xing, Q. Chen, A novel method for photosynthesis measuring using chloroplasts delayed fluorescence, Biosens. Bioelectron. 20 (2004) 454–459.
[4] C.L. Wang, D. Xing, L.Z. Zeng, C.F. Ding, Q. Chen, Effect of artificial acid rain and SO_2 on characteristics of delayed light emission, Luminescence 20 (2005) 51–56.
[5] L.R. Zhang, D. Xing, J.S. Wang, L.Z. Zeng, Q. Li, Light-induced delayed fluorescence as an indicator for UV-B radiation environment stress on plants, J. Optoelectron. Lase, (2007), in press.
[6] J.M. Anderson, N.K. Boardman, Fractionation of the photochemical systems of photosynthesis I chlorophyll contents and photochemical activities of particles isolated from spinach chloroplasts, Biochim. Biophys. Acta. 112 (1996) 403–421.
[7] C.D. Bjorn, A.S. Forsberg, Imaging by delayed light emission (phytoluminography) as a method for detecting damage of the photosynthetic system, Physiol. Plant. 47 (1979) 215–222.
[8] J.S Wang, D. Xing, L.R Zhang, L. Jia, A new principle photosynthesis capacity biosensor based on quantitative measurement of delayed fluorescence in vivo, Biosens. Bioelectron. (2007) in press, doi:10.1016/j.bios.2006.12.007.
[9] C.L. Wang, G.X. Ma, D.W. Fan, R.B. Xia, Spectroscopy research on the origin mechanism for light induced delayed fluorescence of chloroplast, Spectrosc. Spectral Anal. 25 (2005) 1262–1265.
[10] V. Goltsev, I. Zaharieva, P. Lambrev, I. Yordanov, R. Strasser, Simultaneous analysis of prompt and delayed chlorophyll a fluorescence in leaves during the induction period of dark to light adaptation, J. Theor. Biol. 225 (2003) 171–183.
[11] J. Lavorel, Luminescence, in: Govindjee (Ed.), Bioenergetics of Photosynthesis, Academic Press, New York, 1975, pp. 223–317.
[12] K. Turzó, G. Laczkó, Z. Filus, P. Maróti, Quinone-dependent delayed fluorescence from the reaction center of photosynthetic bacteria, Biophys. J. 79 (2000) 14–25.

[13] H.W. Wang, H. Mi, J. Ye, Y. Deng, Y.K. Shen, Low concentrations of $NaHSO_3$ increase cyclic photophosphorylation and photosynthesis in cyanobacterium *Synechocystis* PCC6803, Photosynth. Res. 75 (2003) 151–159.

[14] S. Itoh, N. Murata, Studies on the induction and decay kinetics of delayed light emission in spinach chloroplasts, in: M. Avron (Ed.), Proceedings of the Third International Congress on Photosynthesis, Elsevier, Amsterdam, 1974, pp. 115–126.

[15] X.G. Zhu, Govindjee, N.R. Baker, E. deSturler, D.R. Ort, S.P. Long, Chlorophyll a fluorescence induction kinetics in leaves predicted from a model describing each discrete step of excitation energy and electron transfer associated with Photosystem II, Planta 223 (2005) 114–133.

[16] Y. Munekage, M. Hashimoto, C. Miyake, K.I. Tomizawa, T. Endo, M. Tasaka, T. Shikanai, Cyclic electron flow around photosystem I is essential for photosynthesis, Nature 429 (2004) 579–582.

[17] A.K. Biswal, F. Dilnawaz, K.A.V. David, N.K. Ramaswamy, A.N. Misra, Increase in the intensity of thermoluminescence Q-band during leaf ageing is due to a block in the electron transfer from QA to QB, Luminescence 16 (2001) 309–313.

[18] K. Salem, L.G. van Waasbergen, Photosynthetic electron transport controls expression of the high light inducible gene in the cyanobacterium *Synechococcus elongatus* strain PCC 7942, Plant Cell Physiol. 45 (2004) 651–658.

[19] S.R. Mishra, S.C. Sabat, Photosynthetic electron transport in *Hydrilla verticillata* (L.) is insensitive to methylviologen (paraquat) inhibition, Biochem. Biophys. Res. Commun. 212 (1995) 132–137.

[20] Y. Okegawa, M. Tsuyama, Y. Kobayashi, T. Shikanai, The pgr1 mutation in the rieske subunit of the cytochrome b_6f complex does not affect PGR5-dependent cyclic electron transport around photosystem I, J. Biol. Chem. 280 (2005) 28332–28336.

[21] F. Rappaport, A. Cuni, L. Xiong, R. Sayre, J. Lavergne, Charge recombination and thermoluminescence in photosystem II, Biophys. J. 88 (2005) 1948–1958.

[22] I. Vass, The history of photosynthetic thermoluminescence, Photosynth. Res. 76 (2003) 303–318.